rotational region, the familiar 4+/2+ ratio of 3.3 showing the $I(I+1)$ energy dependence is seen (lower curve). Higher members of this ground-state rotational band are not shown. At higher energies two different intrinsic states are seen and these have been attributed to beta vibrational states (0′+) and gamma vibrational states (2′+) predicted at about these energies by Bohr and Mottelson.[20] (Rotational levels based upon these states are not plotted.) A reason for the apparent sharp drop in energy for the gamma vibrational band in Fm^{254} has not been suggested, however.

The region of particular interest here is that between mass number 216 and 228. Scharff-Goldhaber has suggested that a rather sharp transition in the character of these energy levels occurs between proton numbers 86 (radon) and 88 (radium). However, if our assignment of the 4+ state in Rn^{218} is correct, the behavior of this level through the above region is rather uniform. It cannot be ascertained whether a sharp change in the 2′+ or 0′+ states occurs until the position of these levels in some of the radium isotopes is known. If the downward trend of the 0′+ state in Th^{230} is correct, a sharp break in the position of this level seems rather unlikely. Furthermore, the energy of the first-excited state (broken lines in Fig. 9) is quite smooth throughout this region. Our conclusion, then, is that a sudden change in the character or energy of the levels does not seem likely, although there are not yet sufficient data available to be certain of this conclusion.

Figure 10 is similar to Fig. 9 except that odd-parity levels are considered. The data on the 2− levels are fragmentary, and it is not yet at all certain that any of these levels really have spin and parity 2−, so that they will not be discussed. The 1− states are quite well established, however. In Fig. 10 the lines connect the points for a given element, and there is evidence of a break between the radon and radium isotopes. On the other hand, a break of similar magnitude occurs between radium and thorium, so that probably this only indicates that the position of these levels depends on both the proton and the neutron number. It has been suggested that these 1− levels are due to collective octopole vibrations; however, a satisfactory explanation for the sharp dip in the energy of these levels in the region of radium and thorium has not yet been given.

(University of Pittsburgh and Office of Ordnance Research, U. S. Army, 1957), p. 494.

[20] A. Bohr, Kgl. Danske Videnskab. Selskab, Mat-fys. Medd. **26**, 34 (1952); A. Bohr and B. R. Mottelson, *Beta- and Gamma-Ray Spectroscopy*, edited by Kai Siegbahn (North-Holland Publishing Company, Amsterdam, 1955), p. 474.

PHYSICAL REVIEW VOLUME 119, NUMBER 2 JULY 15, 1960

Electron Pair Production in π^-+d Capture*†

DAVID W. JOSEPH‡
The Enrico Fermi Institute for Nuclear Studies and the Department of Physics, The University of Chicago, Chicago, Illinois
(Received February 25, 1960)

The internal conversion coefficient $\rho(p)=(dW_{2e}/dp)/(dW_\gamma/dp)$ relating the π^-+d capture processes yielding $2n+e^++e^-$ and $2n+\gamma$ is calculated as a function of the n-n relative momentum p. It is found to be a slowly varying function of p, insensitive to the strength of the n-n force. The spectrum of the electron pair energies (or of the momentum p) therefore depends sensitively on the n-n scattering length, just as Watson and Stuart found to be the case for the photon spectrum. Thus, observation of the pair production process is an alternative method of measuring the n-n scattering length.

I. INTRODUCTION

IN the process

$$\pi^-+d\rightarrow 2n+\gamma, \qquad (1.1)$$

the relative frequency of high-energy photons depends on the strength and sign of the n-n interaction.[1] Thus, the more attractive the interaction, the more likely it will be for the two neutrons to be emitted with low relative momentum; and low neutron energy corresponds to high photon energy. An attempt has been made to determine the ^1S n-n scattering length from a measurement of the photon spectrum,[2] but only very wide limits could be set. This scattering length cannot be obtained from n-p or p-p data by the arguments of charge independence or charge symmetry, since it is very sensitive to slight differences in the nucleonic interactions such as may be expected to result from electromagnetic effects. It is, in fact, true that the (effective nuclear) scattering lengths for the n-p and p-p systems are significantly different, being -24f and -16f,[3] respectively; this difference corresponds to a difference in well depth of between one and three per-

* This research was supported principally by a National Science Foundation Predoctoral Fellowship; it was completed under the auspices of the U. S. Atomic Energy Commission.

† A thesis submitted in partial fulfillment of the requirements for the Ph.D. degree in the Department of Physics at the University of Chicago, Chicago, Illinois.

‡ Now at Purdue University, Lafayette, Indiana.

[1] K. Watson and R. Stuart, Phys. Rev. **82**, 738 (1951).

[2] R. Phillips and K. Crowe, Phys. Rev. **96**, 484 (1954).

cent, depending on the well shape assumed,[3] and so is of the order of magnitude to be expected from electromagnetic effects. Thus, as far as the scattering lengths are concerned, charge independence is significantly violated for the physical nucleons; and it is to be expected that a similar violation may occur for charge symmetry. Therefore, the ^1S n-n scattering length is not well known; although unlikely, it is not completely excluded that it could be positive, corresponding to a weakly bound n-n state.

A process from which determination of the n-n scattering length may be more feasible than from (1.1) is

$$\pi^-+d\rightarrow 2n+e^++e^-; \tag{1.2}$$

this process may be looked upon as the production of a virtual photon by π^-+d capture, followed by its internal conversion. In this case, the strength of the n-n interaction can be inferred from the energy spectrum of the electron pairs. Although this pair production process will be less probable than (1.1) by a factor of the order of α, it can readily be observed in a deuterium bubble chamber, thus avoiding the low efficiency inherent in a high-resolution γ-ray spectrometer such as was used in reference 2.

II. CALCULATION

The simplest form of impulse approximation will be used, in which the incoming meson is assumed to interact directly with the superposition of free-proton wave functions given by the expansion

$$\phi_0(x)=\int\phi(p)e^{ip\cdot x}d^3p,$$

where $\phi_0(x)$ is the wave function of the deuteron. More complicated processes involving both neutron and proton[4] will be neglected. The relative π^-—p motion (due to the motion of the proton in the deuteron) will be ignored in the evaluation of the $\pi^-+p\rightarrow n+$virtual γ matrix element. Watson and Stuart[1] have given some discussion of the justification for this; the smallness of the effect is indicated by the fact that a typical proton momentum of the order of $\mu/3$ corresponds to a relative momentum of only about $\mu/20$. Finally, the n-n interaction has been taken into account in only the S-state function, although transitions to final n-n P states will be shown to make a sizable contribution. While it is true that the forces for $T=1$ P-states are rather strong,[5] and so may appreciably modify the photon spectrum for (1.1), we are here concerned with the calculation of the internal conversion coefficient [the ratio of (1.2) to (1.1) for given n-n c.m. energy], which is insensitive to the final-state forces.

The wave function used for the deuteron is

$$\phi_0=N(e^{-\alpha r}-e^{-\beta r})/r, \tag{2.1}$$

with $\alpha=0.232$ f^{-1} and $\beta=7\alpha$. Thus the D-state part of the deuteron function is neglected, in accord with Watson and Stuart's finding[1] that its contribution to the (similar) real-photon production process is negligible. The wave functions used for the n-n system are, for the triplet state,

$$\psi_p{}^t=e^{ip\cdot r}-e^{-ip\cdot r} \tag{2.2}$$

and, for the singlet state, $\psi^s=\psi^{s1}+\psi^{s2}$, with

$$\psi_p{}^{s1}=e^{ip\cdot r}+e^{-ip\cdot r}$$

and

$$\psi_p{}^{s2}=(2/pr)[\sin(pr+\delta)-e^{-\lambda r}\sin\delta-\sin pr]. \tag{2.3}$$

This corresponds to the use of the ^1S wave function $2[\sin(pr+\delta)-e^{-\lambda r}\sin\delta]/pr$, which has been chosen to have the correct asymptotic form and to be finite at the origin. The constant λ was chosen to yield the experimental value of the effective range; that is, so that $r_0=2\int(u^2-v^2)dr=2.74$f, where $v=\sin(pr+\delta)/\sin\delta$ and $u=v-e^{-\lambda r}$. This form for the S-wave function was used for ease of computation; a sample calculation showed that the difference between using this function and the true function for a square well is negligible (the effect of a hard core can be neglected, since the energy of the n-n relative motion is very low for the cases of interest). The phase shift was obtained from the effective range formula,

$$p\cot\delta=-1/a+r_0p^2/2, \tag{2.4}$$

with $r_0=2.65$f (this is the value appropriate to the p-p system; deviations from charge independence here, only a few percent in r_0, are not important).

The matrix element for the process (1.1) can be expressed in the form

$$M_\gamma=(2k)^{-\frac{1}{2}}J_\mu(\mathbf{p},k_\nu)\epsilon^\mu, \tag{2.5}$$

where ϵ^μ is the polarization vector of the photon, k_ν is the four-momentum of the photon (so $k_\nu{}^2=0$), and p is the momentum of one neutron in the c.m. system of the two neutrons. Note that J_μ depends on the nucleon spins in addition to the arguments shown. The matrix element for (1.2) can be written in a similar form:

$$M_{2e}=m(P_{0+}P_{0-})^{-\frac{1}{2}}J_\mu(\mathbf{p},k_\nu')(k_\rho'^2)^{-1}\times\bar{u}_+(P_+)\gamma^\mu u_-(P_-), \tag{2.6}$$

where $P_{\sigma\pm}$ are the four-momenta of the positron and electron, $k_\nu'=P_{\nu+}+P_{\nu-}$ is the four-momentum of the virtual photon, $u_\pm$ are the positron and electron spinors, and m is the electron mass.

The differential probabilities dW_γ/dp and dW_{2e}/dp can be obtained from the expressions (2.5) and (2.6); these probabilities refer to averages over the deuteron

[3] R. G. Sachs, *Nuclear Theory* (Addison-Wesley Publishing Company, Inc., Reading, Massachusetts, 1953), p. 151; J. Blatt and V. Weisskopf, *Theoretical Nuclear Physics* (John Wiley and Sons, Inc., New York, 1952), p. 94.

[4] For example, the process in which the virtual photon is emitted from a pion exchanged between the nucleons.

[5] This is known from the study of cross sections and polarization effects in p-p scattering at high energies; see, e.g., P. Cziffra, M. H. MacGregor, M. J. Moravcsik, and H. P. Stapp, Phys. Rev. **114**, 880 (1959); and J. L. Gammel and R. M. Thaler, Phys. Rev. **107**, 291 (1957).

spin states, and to summations over the neutron, electron, positron, and photon polarizations, over the direction of $\mathbf{p}$, and over electron and positron momenta. The conversion coefficient defined by $\rho(p)=(dW_{2e}/dp)/(dW_\gamma/dp)$ can easily be obtained from the general expressions derived by Kroll and Wada.[6] The mass (i.e., total barycentric energy including rest masses) of the recoiling two-neutron system is $M=2(\mathfrak{M}_n{}^2+p^2)^{\frac{1}{2}}$; the mass of the initial pion-deuteron system is $W=\mathfrak{M}_d+\mathfrak{M}_\pi$. Energy conservation yields

$$W=k_0'+(M^2+\mathbf{k}'^2)^{\frac{1}{2}}. \tag{2.7}$$

Equations (8) of reference 2 now yield[7]

$$\rho(p)=\frac{2\alpha}{3\pi}\int_{2m}^{E}dx\frac{k'}{k}\left(1-\frac{x^2}{W^2+M^2}\right)\left(1-\frac{4m^2}{x^2}\right)^{\frac{1}{2}}\times\left(1+\frac{2m^2}{x^2}\right)\left(\frac{R_T}{x}+\frac{x}{k_0'^2}R_L\right), \tag{2.8}$$

where $E=W-M$ and $x^2=k_\mu'^2$. The quantities R_T and R_L are given by [see Equations (7) of reference 2]:

$$R_T(p)=\frac{\sum\int d\Omega_p[|J_1(\mathbf{p},k_\mu')|^2+|J_2(\mathbf{p},k_\mu')|^2]}{\sum\int d\Omega_p[|J_1(\mathbf{p},k_\mu)|^2+|J_2(\mathbf{p},k_\mu)|^2]},$$
$$R_L(p)=\frac{\sum\int d\Omega_p|J_3(\mathbf{p},k_\mu')|^2}{\sum\int d\Omega_p[|J_1(\mathbf{p},k_\mu)|^2+|J_2(\mathbf{p},k_\mu)|^2]}, \tag{2.9}$$

where the summation signs indicate sums over neutron and deuteron spins. Note that this summation, together with integration over the direction of $\mathbf{p}$, has made the numerators above independent of the directions of $\mathbf{k}$ and $\mathbf{k}'$, so that integrations over the corresponding angles are unnecessary. The x_3 axis has been chosen to lie along the photon momentum ($\mathbf{k}$ or $\mathbf{k}'$).

It is easily found that

$$J_\nu^{s,t}(\mathbf{p},k_\mu)=\text{const}\omega_0\int d^3r\, e^{-i\mathbf{k}\cdot\mathbf{r}/2}\psi_{\mathbf{p}}{}^{s,t*}(\mathbf{r})\times\phi_0(r)\chi_{m'}{}^{s,t\dagger}\langle\mathbf{k},k_0|H_\nu|q=0\rangle\chi_m{}^t, \tag{2.10}$$

where $\chi_m{}^t$ is the spin function for the deuteron, $\chi_{m'}{}^{s,t}$ is the spin function for the two outgoing neutrons, and ω_0 is the pion-deuteron relative wave function evaluated at the origin.[8] The superscripts s and t distinguish between singlet and triplet states for the outgoing neutrons. The quantity $\langle\mathbf{k},k_0|H_\nu|q=0\rangle$ is the matrix element for the process $\pi^-+p\to n+[\gamma]$, expressed in the π^-p c.m. system; the π^-p relative momentum q has been set equal to zero, corresponding to the neglect (mentioned above) of the relatively low velocity of the proton in the deuteron. From reference 9, Eqs. (15), we have

$$\langle\mathbf{k},k_0|\mathbf{H}\cdot\boldsymbol{\varepsilon}|q=0\rangle\propto e^V(-x^2)i\boldsymbol{\sigma}\cdot\boldsymbol{\varepsilon}+ei\frac{\boldsymbol{\sigma}\cdot\mathbf{k}\mathbf{k}\cdot\boldsymbol{\varepsilon}}{x^2-2k_0}, \tag{2.11}$$

to sufficient accuracy, where $e^V(-x^2)=e(1+0.05x^2)$ and the pion mass has been set equal to unity. Thus

$$\sum\int d\Omega_p|J_\nu^{s,t}(\mathbf{p},k_\mu)|^2=F_\nu^{s,t}G^{s,t}, \tag{2.12}$$

where

$$F_{1,2}{}^{s,t}=\text{const}\sum_m\sum_{m'}|\chi_{m'}{}^{s,t\dagger}\langle\mathbf{k},k_0|H_{1,2}|q=0\rangle\chi_m{}^t|^2=B^{s,t}\left[\frac{e(-x^2)}{e}\right]^2,$$

and

$$F_3{}^{s,t}=B^{s,t}[1+k^2/(x^2-2k_0)]^2,$$

$B^{s,t}$ being constants such that $B^t=2B^s$; and

$$G^{s,t}=(1/4\pi)\int d\Omega_p|I^{s,t}|^2, \tag{2.13}$$

where

$$I^s=I^{s1}+I^{s2},$$

with

$$I^{sj}=\int d^3r\,\psi_{\mathbf{p}}{}^{sj}(\mathbf{r})e^{-i\mathbf{k}\cdot\mathbf{r}/2}\phi_0(r)\quad\text{for } j=1,2,$$

and

$$I^t=\int d^3r\,\psi_{\mathbf{p}}{}^t(\mathbf{r})e^{-i\mathbf{k}\cdot\mathbf{r}/2}\phi_0(r).$$

The wave functions ϕ_0, ψ^{s1}, ψ^{s2}, and ψ^t are given by (2.1), (2.2), and (2.3). The quantity G^s will be written as a sum of three terms: $G^s=G^{s11}+G^{s12}+G^{s22}$. Evaluation of these integrals yields

$$G^{s11}=\frac{16\pi^2N^2}{pk}\left\{\left[\left(\frac{1}{A}+\frac{4B}{A^2-B^2}\right)\ln\frac{1+a}{1-a}+\frac{2}{A}\frac{a}{1-a^2}\right]+[A,a\leftrightarrow B,b]\right\},$$
$$G^{s12}=\frac{8\pi N}{pk}h\ln\left(\frac{1+a}{1-a}\frac{1-b}{1+b}\right), \tag{2.14}$$
$$G^{s22}=|h|^2,$$
$$G^t=\frac{16\pi^2N^2}{pk}\left\{\left[\left(-\frac{1}{A}+\frac{4A}{A^2-B^2}\right)\ln\frac{1+a}{1-a}+\frac{2}{A}\frac{a}{1-a^2}\right]+[A,a\leftrightarrow B,b]\right\},$$

[6] N. Kroll and W. Wada, Phys. Rev. **98**, 1355 (1955).
[7] After correction of a numerical error.
[8] In (2.10) through (2.14) it is unnecessary to distinguish between real and virtual photons; therefore the unprimed symbols k_μ and $\mathbf{k}$ have been used throughout.
[9] S. Fubini, Y. Nambu, and V. Wataghin, Phys. Rev. **111**, 329 (1958).

where

$$h=\frac{4\pi N}{pk}\Big\{\Big[(1-\cos\delta)\ln\frac{1-a}{1+a}+2\sin\delta\Big(\arctan\frac{\alpha k}{\alpha^2-p^2-k^2/4}-\arctan\frac{(\alpha+\lambda)k}{(\alpha+\lambda)^2-k^2/4}\Big]-[a,\alpha\leftrightarrow b,\beta]\Big\},$$

$$A=\alpha^2+p^2+k^2/4,\quad B=\beta^2+p^2+k^2/4,$$

$$a=pk/A,\quad b=pk/B.$$

The notation $[A,a\leftrightarrow B,b]$ indicates a term obtained from the preceding term by interchanging A with B, and a with b. From Eqs. (2.9) and (2.12) we have that

$$R_T(p,x)=\frac{G^s(p,x)+2G^t(p,x)}{G^s(p,0)+2G^t(p,0)}\Big[\frac{e(-x^2)}{e}\Big]^2,$$
$$R_L(p,x)=\frac{G^s(p,x)+2G^t(p,x)}{G^s(p,0)+2G^t(p,0)}\frac{1}{2}\Big[1+\frac{k'^2}{x^2-2k_0'}\Big]^2. \quad (2.15)$$

Thus, from (2.8),

$$\rho(p)=\frac{2\alpha}{3\pi}\int_{2m}^{E}\frac{dx}{x}\Big[1-\frac{4m^2}{x^2}\Big]^{\frac{1}{2}}\Big[1+\frac{2m^2}{x^2}\Big]\times\frac{k'}{k}\Big[1-\frac{x^2}{W^2+M^2}\Big]\frac{G^s(p,x)+2G^t(p,x)}{G^s(p,0)+2G^t(p,0)}\times\Big\{\Big[\frac{e(-x^2)}{e}\Big]^2+\frac{x^2}{2k_0'^2}\Big[1+\frac{k'^2}{x^2-2k_0'}\Big]^2\Big\}. \quad (2.16)$$

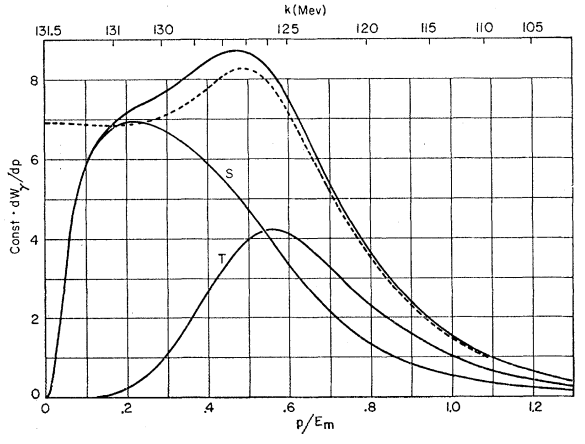

FIG. 1. The distribution dW_γ/dp for emission of real photons. The contributions from singlet and triplet $2n$ states are denoted by S and T, respectively; the unmarked curves are total rates (i.e., singlet plus triplet). The solid curves are for a scattering length of $a_s=-23.7$f, and the dashed curve is for $a_s=-\infty$. $E_m=136.1$ Mev is the maximum value of $E=W-M$ (attained for $p=0$).

In this expression the first term in braces represents the contribution of longitudinal photons. For numerical evaluation, it is convenient to define $\mathfrak{F}(p,x)$ so that

$$\rho(p)=\frac{2\alpha}{3\pi}\int_{2m}^{E}\frac{dx}{x}\Big[1-\frac{4m^2}{x^2}\Big]^{\frac{1}{2}}\Big[1+\frac{2m^2}{x^2}\Big]\mathfrak{F}(p,x). \quad (2.17)$$

Noting that $\mathfrak{F}(p,0)=1$, we can rewrite this as

$$\rho(p)=\frac{2\alpha}{3\pi}\Big\{\int_{2m}^{E}\frac{dx}{x}\Big[1-\frac{4m^2}{x^2}\Big]^{\frac{1}{2}}\Big[1+\frac{2m^2}{x^2}\Big]+\int_0^E\frac{dx}{x}[\mathfrak{F}(p,x)-\mathfrak{F}(p,0)]\Big\} \quad (2.18)$$

where the limit $m\to 0$ has been taken in the second integral since the contribution for $x\sim m$ is negligible there. The first integral can be evaluated analytically, so that

$$\rho(p)=\frac{2\alpha}{3\pi}\Big\{\Big[\ln\frac{1+(1-\xi^2)^{\frac{1}{2}}}{\xi}-\tfrac{1}{6}(5+\xi^2)(1+\xi^2)^{\frac{1}{2}}\Big]+\int_0^E\frac{dx}{x}[\mathfrak{F}(p,x)-\mathfrak{F}(p,0)]\Big\}, \quad (2.19)$$

where $\xi\equiv 2m/E$. The second integrand is relatively small and slowly varying, so that the second integral may easily be evaluated numerically.

The photon spectrum for process (1.1) is easily found to be [see Eq. (2) of reference 6]

$$\frac{dW_\gamma}{dk}=\frac{1}{p}\frac{dW_\gamma}{dp}=\text{const}\,kp[W^2+M^2]\times[G^s(p,0)+2G^t(p,0)]. \quad (2.20)$$

Figure 1 shows the spectrum dW_γ/dp (which is equal to the photon spectrum dW_γ/dk multiplied by p) for

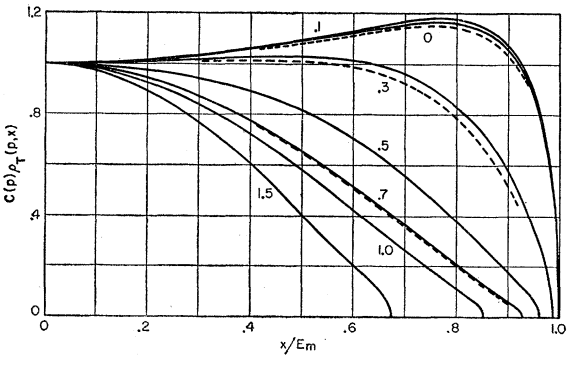

FIG. 2. The transverse component of the conversion coefficient, $\rho_T(p,x)$, multiplied by x, normalized by the function $C(p)\equiv 1/\rho_T(p,0)$. (A factor of x is missing from the ordinate label.) The numbers adjacent to the curves are the values of p. The solid curves are for a scattering length of $a_s=-23.7$f. The adjacent dashed curves shown for several p values are for a scattering length of $-\infty$.

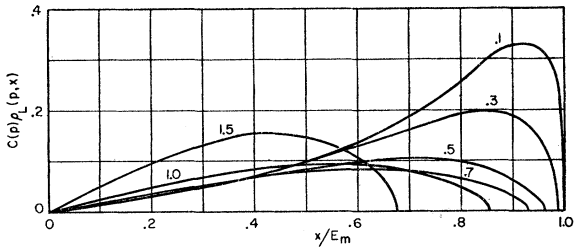

FIG. 3. The longitudinal component of the conversion coefficient, $\rho_L(p,x)$, normalized by the same function $C(p)$ as the curves of Fig. 2. Note that the vertical scale is here expanded by a factor of two compared with that of Fig. 2. The numbers adjacent to the curves are the values of p. These curves are for a scattering length of $a_s=-23.7$f.

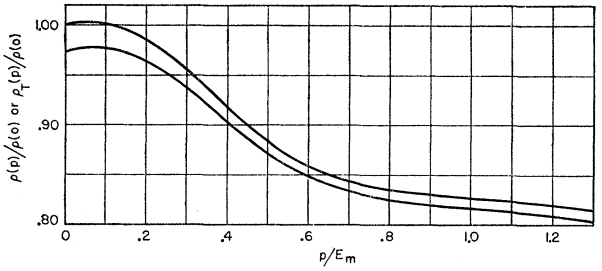

FIG. 4. The conversion coefficient $\rho(p)$ (upper curve) and the portion thereof due to transverse virtual photons, $\rho_T(p)$ (lower curve). These curves are calculated for $a_s=-23.7$f.

an n-n ^1S scattering length of -23.7f (the experimental n-p value), together with the breakdown into singlet and triplet contributions. The total curve for infinite scattering length is also shown, to indicate the sensitivity of the spectrum to the nuclear forces.[10]

Figure 2 indicates the manner in which $x\rho_T(p,x)$, i.e., the transverse portion of the integrand of Eq. (2.16) multiplied by x, varies with x, for various values of p. The dotted curves indicate, for three values of p, the effect of changing the scattering length from -23.7f to infinity; the effect is seen to be small. Figure 3 shows the similar distribution for the longitudinal contribution. Finally, Fig. 4 shows the conversion coefficient $\rho(p)$, obtained by integrating the curves of Figs. 2 and 3 by the method of Eq. (2.19), for the case $a_s=-23.7$f; it is seen to be a slowly varying function.

The conversion coefficient $\rho(p)$ depends only weakly on p (Fig. 4), is only slightly affected by the strength of the n-n force (Fig. 2), and is also largely independent of pion-nucleon processes. The reason for this is the strong peaking of the integrand of (2.16) toward small x values, due to the factor $1/x$. Thus, the first integral[11] of (2.18) is the dominant one, since the factor $\mathfrak{F}(p,x)-\mathfrak{F}(p,0)$ causes the integrand of the second to remain small (in fact, to vanish) as $x\rightarrow 0$. But the first integral is independent of pion physics altogether, depending, in fact, only on the electrodynamics of the process; all dependence on the n-n force, and on the $\pi^-+p\rightarrow n+[\gamma]$ matrix element for longitudinal photons or for transverse photons off the zero-mass shell is contained in the second, relatively small, integral.

[10] It must be noted that the spectra dW_γ/dp obtained from the corresponding curves ($\alpha=-8$ Mev and $\alpha=0$) of Fig. 2 of reference 1 do not agree with Fig. 1; they are relatively lower in the vicinity of $p=0.5$ by 10–20%, and the curve for $a_s=-\infty$ passes through zero at $p=0$, which cannot be correct.

[11] This term corresponds to the "standard value" introduced by R. H. Dalitz and D. R. Yennie [Phys. Rev. **105**, 1598 (1957)] in their work on pion production in electron-proton collisions; this "standard value" corresponds essentially to the Weizsäcker-Williams approximation relating the effects of rapidly moving charges to those of photons.

III. CONCLUSIONS

It has been shown that the energy spectrum of the pairs from $\pi^-+d\rightarrow 2n+e^++e^-$ can be directly related to that of the photons from $\pi^-+d\rightarrow 2n+\gamma$. The relating function $\rho(p)=(dW_{2e}/dp)/(dW_\gamma/dp)$ is given by Eq. (2.19) and displayed in Fig. 4. It is only weakly dependent on the n-n interaction, as is shown by the small displacement of the dotted curves of Fig. 2. As a result, the pair production process can be used to determine the photon spectrum for π^-+d capture, and hence, the scattering length. It will be noted from Fig. 1 that success of the method for the latter purpose depends very much on the accuracy with which it is possible to measure the energy of electron pairs corresponding to small values of p. As a rough estimate of the accuracy of the method, it may be noted that those events having electron-pair energy within one Mev of the maximum are expected to account for about one-sixth of all events, and their number would increase by about one-half if the scattering length were varied from -24f to $-\infty$; so a total of 600 pair events would be expected to yield the scattering length to roughly 20%.

High accuracy in measurement of the scattering length depends on counting the number of events having electron-pair energy very close to the maximum. Since these necessarily form a rather small sample with a correspondingly large statistical error (although its size is very sensitive to the scattering length), great accuracy in the shape of the calculated curves is not necessary. Thus even if the scattering length departs considerably from the value of -24f, the conversion function of Fig. 4, relating the pair spectrum to the photon spectrum will not be significantly affected. This function will also not be significantly affected by the approximations made here of neglecting P-state forces and (mesonic) processes involving both the nucleons of the deuteron, for the reasons given at the end of the preceding section. But the effect of these approximations on the photon spectrum can be quite considerable; a more reliable calculation of the photon spectrum will deserve attention when accurate experiments are carried out. However, it can be shown by use of the closure approximation (see Appendix) that the *total* rate of process (1.1), and, therefore, also of process

(1.2), will not be much affected by these approximations; thus the expressions obtained here should be sufficiently accurate for determination of the scattering length from the ratio of low-p events (where the P-state contribution is negligible) to the total rate.

IV. ACKNOWLEDGMENT

The author wishes to express his thanks to Professor R. H. Dalitz for suggesting this problem and for much helpful discussion concerning it.

APPENDIX

From Fig. 1 it will be noted that the major contribution to either G^s or G^t [see (2.20)] comes from a range in k of only a few percent. Thus, in the integrals for the total rate of process (1.1), which are essentially [see (2.13)]

$$\int kp^2dp\, G^{s,t}(p,0) = \frac{1}{4\pi}\int kd^3p \int d^3rd^3r'[\psi_p{}^{s,t*}(\mathbf{r})e^{i\mathbf{k}\cdot\mathbf{r}/2}\phi_0(r)] \times[\psi_p{}^{s,t}(\mathbf{r}')e^{-i\mathbf{k}\cdot\mathbf{r}'/2}\phi_0(r')], \quad (A.1)$$

it will cause small error to ignore the energy conservation relation and set $k=\text{const}$; since the integrands are very small for large p (see Fig. 1), the upper limit on p can be ignored, and the integral over p extended to infinity. For the singlet case we have $\psi^s(-\mathbf{r})=\psi^s(\mathbf{r})$, so we can write (A.1) as

$$\begin{aligned}\int kp^2dp\, G^s(p,0) &\approx \frac{k}{16\pi}\int d^3p \int d^3rd^3r'[\psi_p{}^{s*}(\mathbf{r})(e^{i\mathbf{k}\cdot\mathbf{r}/2}+e^{-i\mathbf{k}\cdot\mathbf{r}/2})\phi_0(r)] \\ &\times[\psi_p{}^{s}(\mathbf{r}')(e^{-i\mathbf{k}\cdot\mathbf{r}'/2}+e^{i\mathbf{k}\cdot\mathbf{r}'/2})\phi_0(r')] \\ &= \frac{k}{16\pi}\int d^3rd^3r'(e^{i\mathbf{k}\cdot\mathbf{r}/2}+e^{-i\mathbf{k}\cdot\mathbf{r}/2})(e^{-i\mathbf{k}\cdot\mathbf{r}'/2} \\ &+e^{i\mathbf{k}\cdot\mathbf{r}'/2})\phi_0(r)\phi_0(r')\sum_{i=s,t}\int d^3p\,\psi_p{}^{i*}(\mathbf{r})\psi_p{}^{i}(\mathbf{r}') \quad (A.2)\end{aligned}$$

since the term involving $\psi_p{}^{t*}(\mathbf{r})\psi_p{}^{t}(\mathbf{r}')$ contributes nothing, due to the fact that $\psi^t(-\mathbf{r})=-\psi^t(\mathbf{r})$. Now the closure relation for wave functions normalized in the fashion of (2.2) and (2.3) reads

$$\sum_{i=s,t}\int d^3p\,\psi_p{}^{i*}(\mathbf{r})\psi_p{}^{i}(\mathbf{r}')=4(2\pi)^3\delta(\mathbf{r}-\mathbf{r}'). \quad (A.3)$$

Thus we obtain

$$\int kp^2dp\, G^s(p,0)\approx 4\pi^2k\int d^3r\,[1+e^{i\mathbf{k}\cdot\mathbf{r}}]\phi_0{}^2(r) = 4\pi^2k[1+f(k)], \quad (A.4)$$

where

$$f(k)\equiv\int d^3r\,\phi_0{}^2(r)e^{i\mathbf{k}\cdot\mathbf{r}}.$$

The corresponding equation for the triplet case can be obtained in the same fashion, except that now the functions $e^{i\mathbf{k}\cdot\mathbf{r}/2}$ and $e^{-i\mathbf{k}\cdot\mathbf{r}'/2}$ are made antisymmetric in $\mathbf{r}$ and $\mathbf{r}'$. This equation is

$$2\int kp^2dp\, G^t(p,0)\approx 8\pi^2k[1-f(k)]. \quad (A.5)$$

Some appropriate average values must be chosen for the quantity k appearing in (A.4) and (A.5); the medians of the singlet and triplet curves of Fig. 1 should be reasonable choices. These are $k^s=129$ Mev $=0.95$ and $k^t=124$ Mev$=0.91$, where units have been chosen such that the maximum value of E, $E_m\approx\mathfrak{M}_\pi$, is equal to unity. With these values we obtain $[1+f(k^s)]=1.52$ and $2[1-f(k^t)]=0.92$, so that

$$\begin{aligned}\int kp^2dp\, G^s(p,0)&\approx 57, \\ 2\int kp^2dp\, G^t(p,0)&\approx 33.\end{aligned} \quad (A.6)$$

The corresponding values from the curves of Fig. 1 [which are plots of $(4\pi N)^{-2}kp^2G^s(p,0)$ and $2(4\pi N)^{-2}\times kp^2G^t(p,0)$; $(4\pi N)^2=13.07$] are

$$\begin{aligned}\int kp^2dp\, G^s(p,0)&=53, \\ 2\int kp^2dp\, G^t(p,0)&=29.\end{aligned} \quad (A.7)$$

The difference between the values of (A.6) and (A.7) is an estimate of the error involved in the closure approximation. Since the expressions (A.4) and (A.5), obtained by use of the closure approximation, are independent of the n-n force, the size of this error is also an indication that the effect of n-n forces on the *total* rate of process (1.1), or of (1.2), is small.